Inorganica Chimica Acta, *162* (1989) 89–96

Effect of Cation on the Structures, Magnetic Properties and Specific Heats of Salts of Bis(5,6-dihydro-1,4-dithiin-2,3-dithiolato)nickelate(III): the Crystal Structure of $[(CH_3)_4N][Ni(DDDT)_2]$

JANE HANNA WELCH, ROBERT D. BEREMAN*, PHIRTU SINGH
Department of Chemistry, North Carolina State University, Raleigh, NC 27695 (U.S.A.)
DAVID HAASE
Department of Physics, North Carolina State University, Raleigh, NC 27695 (U.S.A.)
WILLIAM E. HATFIELD and MARTIN L. KIRK
Department of Chemistry, University of North Carolina at Chapel Hill, Chapel Hill, NC 27514 (U.S.A.)

(Received February 13, 1989)

Abstract

The structure of the tetramethylammonium salt of $Ni(DDDT)_2^-$ ($DDDT^{2-}$ = 5,6-dihydro-1,4-dithiin-2,3-dithiolate) has been determined by X-ray crystallography. The crystal belongs to the orthorhombic space group *Pbca* with unit cell dimensions a = 10.543(2), b = 13.937(5), c = 27.518(7) Å, Z = 8. The NiS_4 core exhibits square planar coordination with an average Ni–S bond length 2.146(2) Å. The crystal packing can be described as interlocking columns consisting of alternating cations and anions. The columns form a zigzag pattern when viewed down the y axis. The shortest S···S contact is 3.57 Å with a total of four contacts less than 3.8 Å. The X-ray powder diffraction spectrum of this salt showed the presence of only one crystallographic species, while that of the tetrabutylammonium salt indicated the possibility of a third polymorph. Magnetic susceptibility data for $[(CH_3)_4N][Ni(DDDT)_2]$ were fit to the Curie–Weiss law by expanding the Weiss constant as an infinite series. The specific heats of the $[(CH_3)_4N]^+$, $[(C_2H_5)_4N]^+$ and $[(C_4H_9)_4N]^+$ salts of $Ni(DDDT)_2^-$ were measured between 1 and 25 K. Similar specific heats were observed above 4 K but the values differed significantly below this temperature.

Introduction

The first report of an 'organic metal', tetrathiafulvalene-tetracyanoquinodimethane (TTF-TCNQ), appeared fifteen years ago and was the impetus for the massive research effort which has led to the synthesis of organic superconductors. This charge transfer complex exhibited metallic behavior between room temperature and 66 K [1]. The crystal structures of TTF-TCNQ [2], and the superconducting perchlorate [3], hexafluoroarsenate [4], and hexafluorophosphate [5] salts of tetramethyltetraselenafulvalene, $(TMTSF)_2X$, have elucidated many structural features necessary for the conduction of electrons. The requirements for the metallic state, both structural and electronic, have been addressed in several reviews [6–14].

The discovery of the first totally sulfur-based organic superconductor [15], bis(ethylenedithiolotetrathiafulvalenium)rhenate, $(BEDT\text{-}TTF)_2ReO_4$, offered further stimulus to the potential of the 'TTF' framework. The tetrathioethylene subunit is believed to be the key structural feature that allows for the conduction of electrons. We have reported a new 1,2-dithiolene, 5,6-dihydro-1,4-dithiin-2,3-dithiolate ($DDDT^{2-}$), synthesized as the potassium salt, as well as several of its transition metal complexes [16, 17].

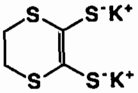

K_2DDDT

The salt, $[(C_2H_5)_4N][Ni(DDDT)_2]$, contains a complex anion which exhibits square planar coordination [16]. A crystallographic analysis showed the anion to have structural features quite similar to BEDT-TTF. Magnetization measurements of the Ni complex showed long-range antiferromagnetic interactions due to the layered structure that allows for some close sulfur–sulfur contacts [16]. This observation has led us to continue to study this system.

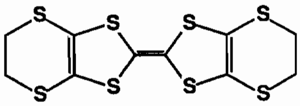

BEDT-TTF

---

*Author to whom correspondence should be addressed.

0020-1693/89/$3.50

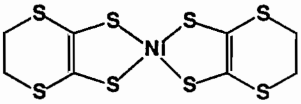

Ni(DDDT)$_2^-$

The significant role of the counterion on crystal structure and thus physical properties has been established. An investigation into the effect of the counterion on the crystal structures of DDDT^{2-} complexes was initiated by the synthesis of the tetrabutylammonium and trimethylammonium salts of Cu(DDDT)$_2^-$ [17]. It was found that the tetraalkylammonium ion affected different crystalline space groups, $P2_1/c$ and $Pnnm$, respectively. A similar study of complexes with dmit^{2-} (2-thioxo-1,3-dithiole-4,5-dithiolate) has yielded highly conductive partially oxidized complexes of nickel with tetraalkylammonium cations as counterions [18–21]. More recently, the reaction of TTF with Ni(dmit)$_2$ has resulted in a complex that is superconducting under pressure [22–25].

In a continuation of this work, two different salts of the bis nickel complex of DDDT^{2-}, the tetramethylammonium and tetrabutylammonium salts, have been synthesized and studied by X-ray crystallography. As was the case with the copper complexes, the crystal of the tetrabutylammonium nickel complex belongs to a monoclinic space group while that of the tetramethylammonium salt exhibits an orthorhombic unit cell. The tetraethylammonium salt shows a monoclinic structure [16]. Another structure of the tetrabutylammonium salt has been reported by Williams *et al.* [26] in which the crystal belongs to the triclinic space group $P\bar{1}$. Because we were unable to duplicate this structure, a brief note [27] contrasting these two polymorphs has been published.

This report details the structure and magnetic properties of the tetramethylammonium salt of Ni(DDDT)$_2^-$. The structural features of the Ni(DDDT)$_2^-$ anion will be compared for the tetramethylammonium and tetrabutylammonium salts. A discussion of magnetic data in relation to crystallographic parameters such as molecular packing and S···S contacts includes all four Ni(DDDT)$_2^-$ structures. In addition, we report the specific heats of the tetramethylammonium, tetraethylammonium, and tetrabutylammonium salts synthesized in our laboratory.

Experimental

Reagents

Potassium 5,6-dihydro-1,4-dithiin-2,3-dithiolate (K$_2$DDDT) was prepared by literature methods and characterized by IR and NMR [16]. Ni(II) chloride hexahydrate was purchased from Matheson, Coleman, and Bell. Tetramethylammonium chloride and acetonitrile were purchased from Aldrich Chemical Company. Methanol was purchased from Fisher Scientific Company. Argon was purchased from Air Products Inc. All chemicals were used without further purification.

Procedures

Elemental analyses were performed by Atlantic Microlabs, Atlanta, GA. The ligand, K$_2$DDDT, was transferred to a reaction flask containing methanol under an argon stream by using standard Schlenk techniques.

Synthesis of [(CH$_3$)$_4$N][Ni(S$_4$C$_4$H$_4$)$_2$]

This complex anion was synthesized with K$_2$DDDT (1.1 g) and NiCl$_2$·6H$_2$O (0.5 g) in methanol by the literature method [16] and precipitated with an excess of tetramethylammonium chloride (0.5 g). The product was recrystallized in acetonitrile to yield 0.2 g (20%) of small green crystals. Melting point (decomposes at 222 °C); IR (KBr): 2910(w), 1475(s), 1420(m), 1365(s), 1280(s), 1165(m), 1120(w), 950(m), 865(m), 775(w), 440(m), 380(m) cm^{-1}. *Anal.* Calc. for NiC$_{12}$H$_{20}$NS$_8$: C, 29.20; H, 4.08; N, 2.84; S, 51.98. Found: C, 29.26; H, 4.07; N, 2.85; S, 52.09%.

Physical Measurements

IR spectra were recorded on a Perkin-Elmer 521 spectrophotometer over the range 4000–300 cm^{-1}.

X-ray powder diffraction spectra were recorded on a Diano XRD-7D diffractometer with Cu Kα radiation, 1° beam slit, medium resolution soller slit, and diffracted beam graphite monochromator. The traces were collected at a 2θ scanning speed of 2°/min. Samples were prepared on glass slides using petroleum jelly.

Magnetic susceptibility data were collected with a Princeton Applied Research Model 155 vibrating-sample magnetometer (VSM) that was operated from zero field to 15 kOe by using procedures described previously and was calibrated with HgCo(NCS)$_4$ [28, 29]. Powdered samples of the calibrant and compound, approximately 150 mg of each, were contained in precision-milled Lucite sample holders. Diamagnetic corrections for the constituent atoms were made by using Pascal's constants, and corrections for temperature-independent paramagnetism were estimated from tabulated data [30–32].

The specific heats of three Ni(DDDT)$_2^-$ salts were measured between 1 and 25 K using a thermal relaxation technique [33]. The samples were greased onto calorimeters constructed from a strain gauge heater [34] and a thick film resistance thermometer [35]. To increase thermal contact some of the samples were placed on a 0.001" thick copper foil. The mass of the calorimeter was about 25 mg and typical sample masses were 8 to 29 mg. The calorimeters were suspended from four 0.002" diameter manganin leads from the mixing chamber of a dilution refrigerator. The calorimeter heat capacity was measured separately as well as the heat capacity of a 515 mg sample of 99.99% indium, to validate the measuring process. The heat capacity of the copper foil, when it was used, was calculated from literature values, and was probably the greatest source of error. Between 1 and 20 K the addendum heat capacity was no more than 25% of the total. The measured indium specific heats agreed with accepted values to within 10%.

Single-crystal X-ray Analysis

A representative crystal was surveyed, and cell dimensions were obtained by a least-squares fit of setting angles of 25 high-angle reflections ($2\theta > 40°$). A data set was collected on a Nicolet R3m/μ diffractometer equipped with a graphite monochromator and copper radiation ($\lambda = 1.54178$ Å). Systematic absences indicated that the crystal belonged to the orthorhombic space group *Pbca* ($0kl$, $k = 2n + 1$; $h0l$, $l = 2n + 1$; $hk0$, $h = 2n + 1$). Two check reflections collected after every 48 reflections revealed no unexpected variation in intensity. Data were corrected for Lorentz and polarization effects. A psi scan was used for an empirical absorption correction that was necessitated by the large absorption coefficient (86.4 cm^{-1}). An isotropic secondary extinction correction was made (secondary extinction coefficient = 2.0×10^{-6}). Atomic scattering factors for all atoms were taken from the International Tables for X-ray Crystallography [36]. Pertinent crystal, data collection and refinement parameters are summarized in Table 1.

The nickel and several sulfur atoms were located by the direct-methods program SOLV of the crystallographic program package SHELXTL [37]. The remaining non-hydrogen atoms were found by conventional difference Fourier techniques to give a trial structure. The structure was refined by the block-diagonal least-squares technique using SHELXTL on a Data General Microeclipse computer. The quantity minimized was $\Sigma w(\Delta F)^2$, where $w = 1/(\sigma_F^2 + 0.00067F^2)$. The non-hydrogen atoms were refined with anisotropic temperature factors. The hydrogen atoms were placed in calculated positions 0.96 Å away from the attached carbon atom and were not refined. A final difference Fourier map revealed no missing or misplaced electron density.

A thermal ellipsoid diagram of the anion was created by using the SHELXTL graphics package. The stereoview of molecular packing was plotted by using the program ORTEP [38]. See also 'Supplementary Material'.

TABLE 1. Single crystal X-ray crystallographic analysis

Crystal parameters	
Formula	$NiC_{12}H_{20}NS_8$
Molecular weight	493.51
Crystallization medium	acetonitrile
Crystal size (mm)	$0.45 \times 0.35 \times 0.35$
Crystal color	green
Crystal habit	needle
Cell dimensions	$a = 10.543(2)$ Å
	$b = 13.937(5)$ Å
	$c = 27.518(7)$ Å
Volume	4043(2) $Å^3$
Space group	*Pbca*
Molecules/unit cell	8
Density calc. (g/cm^3)	1.62
$F(000)$	2040
Data collection parameters	
Radiation	Cu Kα
Temperature	298 K
2θ range	3–115°
Scan type	θ–2θ
Scan speed	variable, 4–29.3°/min
Octants collected	*hkl*
No. reflections collected	3289
No. reflections used ($I > 2.5\sigma(I)$)	2167
Background measurement	1/2 of total scan time at beginning and end of each scan
Linear absorption coefficient	86.4 cm^{-1}
Refinement parameters[a]	
Final R index	$R = 0.052$
	$R_w = 0.070$
Goodness of fit	1.96
Largest shift/e.s.d.	0.1
Data/parameter ratio	10.2

[a] The data fit criteria (based on reflections having $I > 2\sigma(I)$) were: $R = \Sigma \| F_o| - |F_c \| / \Sigma F_o$; $R_w = [\Sigma w(\Delta F)^2 / \Sigma F_o{}^2]^{0.5}$; $GOF = \Sigma(w[\| F_o| - |F_c \|]^2 / [N_o - N_v])^{0.5}$.

Results and Discussion

The structure and numbering scheme of the $Ni(DDDT)_2^-$ anion are shown in Fig. 1. The four sulfurs surround the nickel atom in square planar coordination with an average S–Ni–S angle of 90.0(1)°. The average Ni–S and C=C bond lengths in the tetramethylammonium salt are 2.146(2) and 1.354(8) Å, respectively. The corresponding values in the tetrabutylammonium salt are 2.137(3) and 1.37(1) Å, respectively. The twelve C–S bonds average to the same value in both salts (1.75 Å). However, if the four C–S bonds in the five-membered ring formed through coordination with nickel are averaged separately from the others, the values are

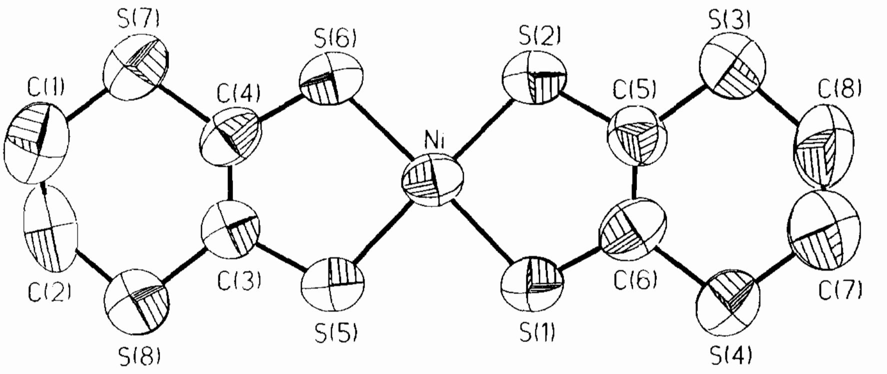

Fig. 1. Structure of $Ni(DDDT)_2^-$ showing the numbering scheme. Hydrogen atoms are not shown. Thermal ellipsoids are drawn at the 50% probability level.

1.724(6) and 1.764(9) Å for the tetramethylammonium salt. This is less apparent in the tetrabutylammonium salt where the averages are 1.72(1) and 1.76(2) Å, because of higher thermal motion. The shorter C–S bond lengths are indicative of partial double bond character. This electron delocalization in transition metal dithiolenes creates difficulty in the assignment of an oxidation state to a metal, and is only one feature which has made these complexes the subject of intense study [39–41]. Differences in the Ni–S and C=C bond lengths can only be explained as the result of steric interactions in the solid. Even though they do exist, the values are consistent with electron delocalization within the coordination ring, i.e. the longer Ni–S bond length corresponds to a shorter C=C distance and vice versa. Bond lengths, bond angles and atomic coordinates are given in Tables 2, 3, and 4 respectively.

The average C–C single bond length in the outer ring of the ligand is highly uncharacteristic (1.39(1) and 1.37(3) Å for the tetramethylammonium and tetrabutylammonium salts, respectively). While the individual values for $[(CH_3)_4N][Ni(DDDT)_2]$ are close to the average, the two values for $[(C_4H_9)_4N]$-$[Ni(DDDT)_2]$ differ significantly (1.23(3) and 1.50(2) Å). These discrepancies are the result of thermal motion and possibly disorder, evidenced in the isotropic temperature factors (Table 4). Similar structural parameters have been observed previously and are not of major concern [42, 43]. However, the orientation of the $-CH_2CH_2-$ fragment in the solid state has been of interest for square planar structures containing the $DDDT^{2-}$ ligand. In the tetramethylammonium salt, both fragments lie to one side of the mean plane of the anion while in the tetrabutylammonium salt, both fragments are puckered with one carbon lying above and one carbon lying below the mean plane. A discussion of the orientation has been presented and was found to be random, most likely the result of steric interactions in the crystal lattice [43]. The above examples support this conclusion.

TABLE 2. Bond lengths (Å)

Ni–S(1)	2.148(2)	Ni–S(2)	2.139(2)
Ni–S(5)	2.145(2)	Ni–S(6)	2.153(2)
S(1)–C(6)	1.720(6)	S(2)–C(5)	1.729(6)
S(3)–C(5)	1.750(5)	S(3)–C(8)	1.778(9)
S(4)–C(6)	1.758(6)	S(4)–C(7)	1.786(8)
S(5)–C(3)	1.716(5)	S(6)–C(4)	1.731(5)
S(7)–C(1)	1.771(8)	S(7)–C(4)	1.742(6)
S(8)–C(2)	1.769(8)	S(8)–C(3)	1.756(5)
C(1)–C(2)	1.42(1)	C(3)–C(4)	1.361(7)
C(5)–C(6)	1.347(8)	C(7)–C(8)	1.36(1)
N–C(9)	1.46(1)	N–C(10)	1.47(1)
N–C(11)	1.50(1)	N–C(12)	1.43(1)

TABLE 3. Bond angles (°)

S(1)–Ni–S(2)	91.6(1)	S(1)–Ni–S(5)	88.1(1)
S(2)–Ni–S(5)	175.7(1)	S(1)–Ni–S(6)	178.7(1)
S(2)–Ni–S(6)	89.0(1)	S(5)–Ni–S(6)	91.3(1)
Ni–S(1)–C(6)	103.9(2)	Ni–S(2)–C(5)	104.1(2)
C(5)–S(3)–C(8)	101.3(4)	C(6)–S(4)–C(7)	103.9(4)
Ni–S(5)–C(3)	104.3(2)	Ni–S(6)–C(4)	104.3(2)
C(1)–S(7)–C(4)	99.6(4)	C(2)–S(8)–C(3)	105.3(3)
S(7)–C(1)–C(2)	117.5(6)	S(8)–C(2)–C(1)	119.7(7)
S(5)–C(3)–S(8)	113.9(3)	S(5)–C(3)–C(4)	120.4(4)
S(8)–C(3)–C(4)	125.5(4)	S(6)–C(4)–S(7)	115.4(3)
S(6)–C(4)–C(3)	119.1(4)	S(7)–C(4)–C(3)	125.4(4)
S(2)–C(5)–S(3)	115.2(3)	S(2)–C(5)–C(6)	119.8(4)
S(3)–C(5)–C(6)	124.9(4)	S(1)–C(6)–S(4)	114.6(3)
S(1)–C(6)–C(5)	120.3(4)	S(4)–C(6)–C(5)	125.1(4)
S(4)–C(7)–C(8)	124.0(7)	S(3)–C(8)–C(7)	122.6(7)
C(9)–N–C(10)	112.5(7)	C(9)–N–C(11)	105.6(6)
C(10)–N–C(11)	113.1(6)	C(9)–N–C(12)	107.8(8)
C(10)–N–C(12)	110.4(8)	C(11)–N–C(12)	107.1(9)

The counterion exhibits the expected tetrahedral structure with an average C–N–C angle of 109.4(9)°. The four N–C bonds have an average length of

TABLE 4. Atomic coordinates (×10^4) and isotropic thermal parameters (Å^2 × 10^3)

	x	*y*	*z*	*U*[a]
Ni	5030(1)	2822(1)	1273(1)	32(1)
S(1)	4256(2)	4247(1)	1291(1)	48(1)
S(2)	4433(2)	2625(1)	537(1)	45(1)
S(3)	2905(2)	3692(1)	−173(1)	62(1)
S(4)	2678(2)	5445(1)	661(1)	61(1)
S(5)	5757(1)	3066(1)	1991(1)	38(1)
S(6)	5777(2)	1384(1)	1268(1)	41(1)
S(7)	7491(2)	244(1)	1879(1)	55(1)
S(8)	7604(2)	2169(1)	2632(1)	61(1)
C(1)	7533(11)	198(6)	2522(3)	106(4)
C(2)	8093(9)	987(6)	2771(3)	96(4)
C(3)	6645(5)	2062(4)	2113(2)	33(2)
C(4)	6639(5)	1304(4)	1801(2)	34(2)
C(5)	3621(5)	3669(4)	400(2)	6(2)
C(6)	3527(5)	4369(4)	736(2)	36(2)
C(7)	2674(12)	5629(6)	18(3)	117(5)
C(8)	2967(12)	4937(7)	−312(3)	113(5)
N	5043(4)	8009(4)	1229(2)	45(2)
C(9)	6370(8)	8233(7)	1129(4)	104(4)
C(10)	4463(10)	8688(6)	1573(3)	99(4)
C(11)	5035(10)	6993(7)	1410(4)	120(5)
C(12)	4377(14)	8019(13)	778(4)	197(8)

[a] Equivalent isotropic *U* defined as one-third of the trace of the orthogonalized U_{ij} tensor.

1.46(1) Å. Similar to the carbons in the $-CH_2CH_2-$ fragment of the ligand, the carbons in the tetramethylammonium cation exhibit higher thermal motion that results in larger deviations in bond lengths and angles.

A stereoview of the unit cell packing of the tetramethylammonium salt viewed down the *b* axis (Fig. 2) shows the anions forming a zigzag pattern with overlap in the periphery of the ligand. The anions lie parallel to one beneath them and with the cations removed, the anions appear to stack. Actually, these 'stacks' consist of alternating cations and anions and should be termed columns. The anions are not planar in this view, but are tilted toward or away from the observer. The anions in a column are tilted similarly. However, the interlocking among stacks is odd because the anions in some columns are tilted in opposite directions. The space between the anions created by the presence of the cation allows for overlap of these outer rings despite the opposing tilts. The closest Ni···Ni contact is 8.57 Å.

The shortest S···S contact in this crystal structure is 3.57 Å and occurs between S5 and S7′. There are a total of eight contacts less than 4.50 Å. These occur between anions in different stacks in the overlap region and across the gap to anions in different zigzag segments. The presence of a cation between anions in the columns disallows close S···S contacts among parallel anions. As expected, more S···S contacts below the cutoff value of 4.50 Å are seen in the structure of the tetramethylammonium salt than the tetrabutylammonium and tetraethylammonium salts (Table 5). The report of the $P\bar{1}$ structure of $[(C_4H_9)_4N][Ni(DDDT)_2]$ contained only three contacts less than 5 Å. These are also shown in Table 5 for comparison.

The magnetic data for $[(CH_3)_4N][Ni(DDDT)_2]$ appeared to indicate the presence of two crystalline forms. The possibility of more than one structural

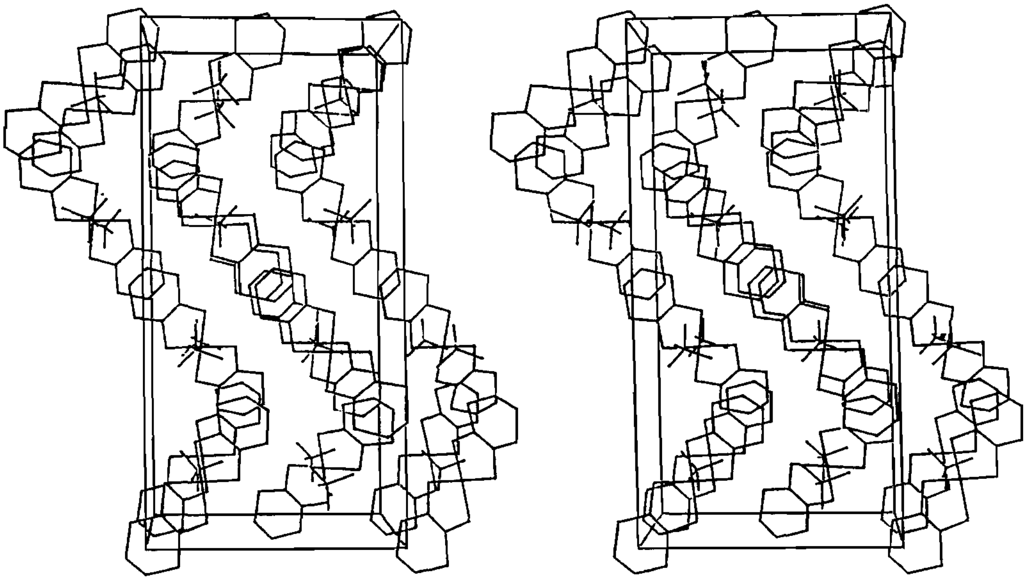

Fig. 2. Stereoview of the unit cell packing for $[(CH_3)_4N][Ni(DDDT)_2]$.

TABLE 5. S···S contacts for $Ni(DDDT)_2^-$ salts (Å)[a]

$[(CH_3)_4N]^+$		$[(C_2H_5)_4N]^{+,b}$	
S(5)–S(7)′	3.57	S(4)–S(3)′	3.98
S(5)–S(8)′	3.70	S(3)–S(4)′	3.98
S(3)–S(6)′	3.76	S(4)–S(4)′	4.25
S(2)–S(4)′	3.78	S(3)–S(3)′	4.49
S(1)–S(7)′	4.04		
S(2)–S(3)′	4.22		
S(4)–S(6)′	4.22		
S(1)–S(8)′	4.49		
$[(C_4H_9)_4N]^{+,c}$		$[(C_4H_9)_4N]^{+,d}$	
S(7)–S(7)′	3.43	S(13)–S(14)′	4.75
S(8)–S(1)′	3.88	S(12)–S(13)′	4.98
S(8)–S(4)′	4.33	S(11)–S(14)′	5.00

[a]Values ≤4.50 Å. [b]Ref. 16. [c]Ref. 27. [d]Ref. 26, values ≤5.00 Å.

form was reasonable in light of the fact that two polymorphs are reported for $[(C_4H_9)_4N]$-$[Ni(DDDT)_2]$ [26, 27]. Therefore, we decided to obtain a powder diffraction pattern of the sample used in collection of magnetic data and compare that to one generated from the atomic coordinates and cell constants of the refined structure. There was a peak to peak correlation for the two powder patterns for $3^\circ < 2\theta < 50^\circ$. No peaks of significant intensity were observed above 50°.

While examining the tetramethylammonium salt by X-ray powder diffraction we decided to investigate a sample of the tetrabutylammonium salt also. The magnetic data did not present problems in this case and each crystal examined was found to be identical by X-ray crystallography. However, we were interested to see if a small impurity of the $P\bar{1}$ form existed in our sample that did not affect the magnetic measurements. Again, the experimental pattern was compared to ones generated from the atomic coordinates and cell constants of both structural forms, $P\bar{1}$ and $P2_1/c$. We were surprised to find the sample pattern did not match peak for peak either generated pattern. For $2\theta < 10^\circ$ there was no correlation. For $10^\circ < 2\theta < 19^\circ$, the patterns from the sample and the $P2_1/c$ structure matched. Beyond 19°, there was no correlation. No peaks were evident for $2\theta > 30^\circ$. These results are very interesting and indicate the possibility of yet another crystalline form. It should be noted that the sample used to obtain the powder pattern was not the same sample used for crystallographic structure analysis as it was no longer available.

Magnetic susceptibility data for $[(CH_3)_4N]$-$[Ni(DDDT)_2]$ shows evidence of complicated magnetic behavior (Fig. 3). A plot of the magnetic moment as a function of temperature clearly shows enhanced magnetic interaction compared to the tetrabutylammonium salt where weak antiferromagnetic interactions were observed [27]. Attempts were made to fit the data to the expansions of Lines [44] and Baker *et al.* [45], as well as a two-dimensional network based on the CAMS program [46]. None of these proved successful. An excellent fit to the data was accomplished by using the Curie–Weiss law and expanding the Weiss constant as an infinite series described by the generating function

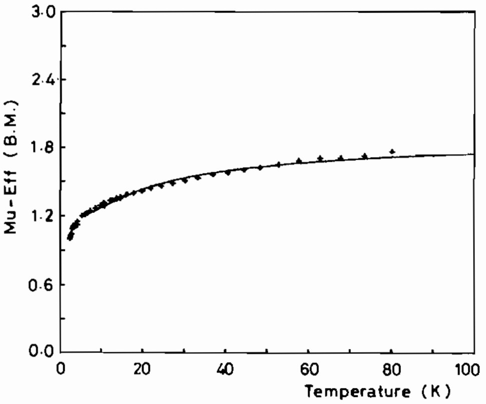

Fig. 3. Magnetic moment of $[(CH_3)_4N][Ni(DDDT)_2]$.

$$\theta = \sum_{n=0}^{\infty} a_n T^{-n}$$

It was found that the first three terms in the series were all that was necessary to adequately fit the data. The best fit parameters are $g = 2.18$, $a_1 = -17.5$, $a_2 = 58.4$, $a_3 = -23.5$.

The magnetic behavior of $[(CH_3)_4N][Ni(DDDT)_2]$ may be due to a contraction of the crystal lattice upon cooling of the sample. This would result in increased sulfur–sulfur π overlap and concomitant enhancement of the magnetic interactions. However, no evidence of a phase transition was observed in the susceptibility, and the magnetization at 4 K displays linear behavior. The crystal structure indicates that multiple exchange pathways exist, and next-nearest-neighbor interactions are possible. If the dominant interactions give rise to a low-dimensional magnetic system, then a band of energy levels with a range of spin multiplicities will exist. The decrease in magnetic moment at low temperatures is a result of depopulating those of higher spin multiplicities. In view of the low symmetry of the structure, the problem of extracting meaningful exchange constants and determining the energy levels from the a_ns would be formidable tasks and these problems remain to be solved.

Magnetic exchange interactions in the tetramethylammonium and tetrabutylammonium salts of $Ni(DDDT)_2^-$ have been difficult to quantify due to the corresponding difficulty in determining exchange pathways between magnetic sites. Exchange between any two metal sites are mediated through short S•••S contacts on the DDDT^{2-} ligands. The strongest interactions would most probably utilize the π orbitals of sulfur atoms directly bound to Ni. In Table 5, we can see that the tetramethylammonium salt possesses four such contacts less than 3.8 Å while for the tetrabutylammonium salt, the shortest contact fitting the above criterium occurs at 3.88 Å. The structure of the tetrabutylammonium salt contains anions associated into pairs yet there are no close S•••S contacts between anions in a pair due to a large separation created by the cations. The contacts listed correspond to sulfurs of different pairs [27]. Based solely on the S•••S contacts, it would be expected that the tetramethylammonium salt, with its more compact structure, would display enhanced magnetic interactions over the tetrabutylammonium salt. The magnetic data support this conclusion.

In contrast, the four contacts less than 4.50 Å in the tetraethylammonium salt occur between sulfurs in the periphery of the ligand yet the magnetic data suggest long-range magnetic ordering. This is due to the layered structure of the anions [16]. The shortest S•••S distance for the $P\bar{1}$ structure of $[(C_4H_9)_4N][Ni(DDDT)_2]$ is 4.75 Å, and as above, occurs between sulfurs in the outer ring of the ligand. The structure does exhibit stacking along the *a* axis and the contacts listed occur among anions in the stacks. However, there are also anions which lie perpendicular to these stacks creating a non-uniform array of anions. Here, magnetic measurements indicate simple paramagnetic behavior [26]. This is not surprising in view of the crystal packing and lack of shorter S•••S contacts. From these examples, it can be concluded that a motif of anions in a crystal conducive to magnetic interactions, i.e. stacks or sheets, or close S•••S contacts alone are not sufficient criteria for magnetic ordering. However, the combination can lead to exciting and interesting magnetic behavior of complex salts.

We measured the specific heat of three $Ni(DDDT)_2^-$ salts: tetramethylammonium, tetraethylammonium, and tetrabutylammonium, as shown in Fig. 4. Since the three salts share the same anion and the cations each have tetrahedral symmetry they should have similar specific heats. The specific heats are similar above 4 K but differ significantly at lower temperatures. The specific heat of the tetraethylammonium salt is proportional to T^3 at low temperatures giving a Debye temperature of 46 K, assuming 3 degrees of freedom per molecular unit. There is no evidence of an additional contribution to the specific heat either due to conduction processes, the magnetic ordering we reported earlier [16], or orientational ordering of the cations.

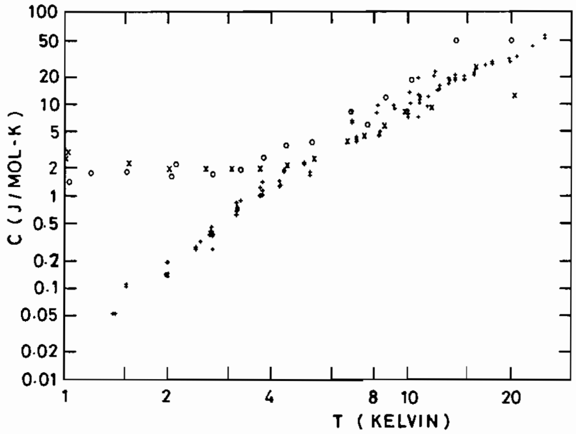

Fig. 4. Specific heat data for tetraalkylammonium salts of $Ni(DDDT)_2^-$: ×, tetramethylammonium; +, tetraethylammonium; ○, tetrabutylammonium.

The tetramethylammonium and tetrabutylammonium salts also show no sharp transitions, but the specific heats are relatively temperature independent below 4 K. The cause of this behavior is not confirmed but we suggest that this is the high temperature tail of a magnetic specific heat anomaly which peaks below 1 K.

Supplementary Material

Tables of anisotropic temperature factors and hydrogen coordinates (2 pages); a listing of calculated and observed structure factors (17 pages) are available from the authors on request.

Acknowledgements

We wish to thank Dr Sterling B. Weed for collection and discussion of X-ray powder diffraction spectra and the National Science Foundation for funds toward upgrading our diffractometer (Grant CHE-8307022). We also thank L. N. Yadon and A. P. Short for help with the specific heat measurements. This work was supported by the donors of the Petroleum Research Fund, administered by the American Chemical Society.

References

1 J. Ferraris, D. O. Cowan, V. Walatka and J. H. Perlstein, *J. Am. Chem. Soc., 95* (1973) 948.
2 T. J. Kistenmacher, T. E. Phillips and D. O. Cowan, *Acta Crystallogr., Sect. B, 30* (1974) 763.
3 K. Bechgaard, K. Carneiro, F. B. Rasmussen, M. Olsen, G. Rindorf, C. S. Jacobsen, H. J. Pedersen and J. C. Scott, *J. Am. Chem. Soc., 103* (1981) 2440.

4 F. Wudl, *J. Am. Chem. Soc., 103* (1981) 7064.

5 N. Thorup, G. Rindorf, H. Soling and K. Bechgaard, *Acta Crystallogr., Sect. B, 37* (1981) 1236.

6 M. L. Khidekel and E. I. Zhilyaeva, *Synth. Met., 4* (1981) 1.

7 A. F. Garito and A. J. Heegar, *Acc. Chem. Res., 7* (1974) 232.

8 F. Wudl, *Acc. Chem. Res., 17* (1984) 227.

9 J. M. Williams, *Prog. Inorg. Chem., 33* (1985) 183.

10 P. M. Chaikin and R. L. Greene, *Phys. Today, 39* (1986) 24.

11 R. L. Greene and P. M. Chaikin, *Physica B + C, 126* (1984) 431.

12 R. L. Greene and G. B. Street, *Science, 226* (1984) 651.

13 D. Jérôme and H. J. Schulz, *Adv. Phys., 31* (1982) 299.

14 J. M. Williams, M. A. Beno, H. H. Wang, P. C. Leung, T. J. Emge, U. Geiser and K. D. Carlson, *Acc. Chem. Res., 18* (1985) 261.

15 S. S. P. Parkin, E. M. Engler, R. R. Schumaker, R. Lagier, V. Y. Lee, J. C. Scott and R. L. Greene, *Phys. Rev. Lett., 50* (1983) 270.

16 C. T. Vance, R. D. Bereman, J. Bordner, W. E. Hatfield and J. H. Helms, *Inorg. Chem., 24* (1985) 2905.

17 C. T. Vance, *Ph.D. Thesis,* North Carolina State University, 1985.

18 L. Valade, P. Cassoux, A. Gleizes and L. Interrante, *J. Phys. Colloq., 44* (1983) C3-1183.

19 L. Valade, M. Bousseau, A. Gleizes and P. Cassoux, *J. Chem. Soc., Chem. Commun.,* (1983) 110.

20 R. Kato, T. Mori, A. Kobayashi, Y. Sasaki and H. Kobayashi, *Chem. Lett.,* (1984) 1.

21 L. Valade, J.-P. Legros, M. Bousseau, P. Cassoux, M. Garbauskas and L. V. Interrante, *J. Chem. Soc., Dalton Trans.,* (1985) 783.

22 P. Cassoux, L. Valade, J.-P. Legros, L. Interrante and C. Roucau, *Physica B + C, 143* (1986) 313.

23 P. Cassoux, L. Valade, M. Bousseau, J.-P. Legros, M. Garbauskas and L. Interrante, *Mol. Cryst. Liq. Cryst., 120* (1985) 377.

24 M. Bousseau, L. Valade, J.-P. Legros, P. Cassoux, M. Garbauskas and L. V. Interrante, *J. Am. Chem. Soc., 108* (1986) 1908.

25 L. Brossard, M. Ribault, L. Valade and P. Cassoux, *Physica B + C, 143* (1986) 378.

26 A. J. Schultz, H. H. Wang, L. C. Soderholm, T. L. Sifter, J. M. Williams, K. Bechgaard and M. Whangbo, *Inorg. Chem., 26* (1987) 3757.

27 J. H. Welch, R. D. Bereman and P. Singh, *Inorg. Chem., 27* (1988) 3680.

28 P. J. Corvan, W. E. Estes, R. R. Weller and W. E. Hatfield, *Inorg. Chem., 19* (1980) 1297.

29 D. B. Brown, V. H. Crawford, J. W. Hall and W. E. Hatfield, *J. Phys. Chem., 81* (1977) 1303.

30 B. N. Figgis and J. Lewis, in J. Lewis and R. G. Wildins (eds.), *Modern Coordination Chemistry,* Interscience, New York, 1960, Ch. 6, p. 403.

31 E. König, *Magnetic Properties of Transition Metal Compounds,* Springer, West Berlin, 1966.

32 R. R. Weller and W. E. Hatfield, *J. Chem. Educ., 56* (1979) 652.

33 R. Bachman, F. J. DiSalvo, T. H. Geballe, R. L. Greene, R. E. Howard, C. N. King, H. C. Hirsch, K. N. Lee, R. E. Schwall, H.-U. Thomas and R. B. Zubeck, *Rev. Sci. Instrum., 43* (1972) 205.

34 D. Moy and A. C. Anderson, *Cryogenics, 23* (1983) 330.

35 Q. Li, C. H. Watson, R. G. Goodrich, D. G. Haase and H. Lukefahr, *Cryogenics, 26* (1986) 467.

36 *International Tables for X-ray Crystallography,* Vol. IV, Kynoch, Birmingham, U.K., 1974, pp. 71–102.

37 *SHELXTL,* X-ray Instruments Group, Nicolet Instrument Corp., Madison, WI, 1983.

38 C. K. Johnson, *ORTEP-II,* A Fortran thermal-ellipsoik plot program for crystal structure illustrations, *ORNL-5138,* National Technical Information Service, Springfield, VA, 1976.

39 J. A. McCleverty, *Prog. Inorg. Chem., 10* (1968) 49.

40 R. P. Burns and C. A. McAuliffe, *Adv. Inorg. Chem. Radiochem., 22* (1979) 303.

41 G. N. Schrauzer, *Transition Met. Chem. (NY), 4* (1968) 299.

42 J. H. Welch, R. D. Bereman and P. Singh, *Inorg. Chem., 27* (1988) 2862.

43 J. H. Welch, R. D. Bereman and P. Singh, *Inorg. Chim. Acta, 163* (1989) in press.

44 M. E. Lines, *J. Phys. Chem. Solids, 31* (1970) 101.

45 G. A. Baker, H. F. Gilbert, J. E. Rushbrooke and G. S. Rushbrooke, *Phys. Lett., 25A* (1967) 207.

46 R. R. Weller, *Ph.D. Thesis,* University of North Carolina-Chapel Hill, 1979.